Dynamics of Membrane Penetration of the Fluorescent 7-Nitrobenz-2-Oxa-1,3-Diazol-4-yl (NBD) Group Attached to an Acyl Chain of Phosphatidylcholine

Daniel Huster,* Peter Müller,† Klaus Arnold,* and Andreas Herrmann†

*Institute of Medical Physics and Biophysics, University of Leipzig, D-04103 Leipzig; and †Humboldt-University Berlin, Institute of Biology/Biophysics, D-10115 Berlin, Germany

ABSTRACT Location and dynamic reorientation of the fluorophore 7-nitrobenz-2-oxa-1,3-diazol-4-yl (NBD) covalently attached to a short (C6) or a long (C12) *sn2* acyl chain of a phosphatidylcholine molecule was investigated by fluorescence and solid-state NMR spectroscopy. ^{2}H NMR lipid chain order parameters indicate a perturbation of the phospholipid packing density in the presence of NBD. Specifically, a decrease of molecular order was found for acyl chain segments of the lower, more hydrophobic region. Molecular collision probabilities determined by ^{1}H magic angle spinning nuclear Overhauser enhancement spectroscopy indicate a highly dynamic reorientation of the probe in the membrane due to thermal fluctuations. A broad distribution of the fluorophore in the lipid bilayer is observed with a preferential location in the upper acyl chain/glycerol region. The distribution of the NBD group in the membrane is quite similar for both the long- and the short-chain analog. However, a slight preference of the NBD group for the lipid-water interface is found for C12-NBD-PC in comparison with C6-NBD-PC. Indeed, as shown by dithionite fluorescence assay, the long-chain analog reacts more favorably with dithionite, indicating a better accessibility of the probe by dithionite present in the aqueous phase. Forces determining the location of the fluorophore in the lipid water interface are discussed.

INTRODUCTION

In recent years intracellular trafficking of lipids has become a field of broad interest in cell biology. To follow the destiny of lipids, in particular of phospho- and glycolipids, various fluorescent analogs of those lipids have been synthesized and applied. Mostly analogs have been used that bear a short-chain fatty acid residue in one of the two *sn*-positions, usually the *sn2*-position, while a long fatty acid residue is on the other position. Typically, the fluorescent moiety is linked to the short-chain residue such as, for instance, glyco- and phospholipid analogs with a fluorescent 7-nitrobenz-2-oxa-1,3-diazol-4-yl (NBD)-labeled C6 (caproyl) or C12 (dodecanoyl) chain in the *sn2*-position and a palmitoyl or myristoyl residue in the *sn1*-position (see Fig. 1). Those analogs can be easily incorporated into membranes and have been used to assess the trans-bilayer redistribution of lipids across the plasma membrane and various intracellular membranes of eukaryotic and prokaryotic cells (Hrafnsdottir et al., 1997; Tang et al., 1996; Smeets et al., 1994; Comfurius et al., 1990; Pomorski et al., 1996, 1999; Connor et al., 1990, 1994; Colleau et al., 1991). To this end, for example, their back-exchange to bovine serum albumin (BSA) or the conversion of their NBD moiety into a nonfluorescent group due to the chemical reaction with the nonpermeant dithionite have been employed (Pomorski et al., 1994, 1995; McIntyre and Sleight, 1991). C6-NBD-labeled analogs can be more easily incorporated into membranes as well as back-extracted to BSA due to their shorter chain in the *sn2*-position as opposed to C12-NBD analogs. From these properties, it is generally believed that C12-NBD analogs reflect more appropriately the respective endogenous lipid counterparts that, e.g., cannot be extracted by BSA.

From fluorescence quenching by spin-labeled phospholipids, it has been concluded that the polar properties of the NBD group attached to phospholipid chains causes a looping back of the fluorescent moiety toward the membrane surface (Chattopadhyay and London, 1987). No difference of the average localization in the membrane of the NBD group between C6-NBD-PC and C12-NBD-PC has been found. However, this fluorescence-quenching approach did not allow assessment of the dynamical behavior of the localization of the NBD group parallel to the membrane normal and its dependence on the attachment site of the NBD moiety on the flexible chain. Furthermore, there is disagreement about the exact localization of the NBD group in the lipid-water interface. Although the spin probe quenching assay suggests a localization of the NBD group in the more hydrophobic glycerol/upper chain region (Chattopadhyay and London, 1987), analysis of fluorescence properties in various dielectric media led to the conclusion that the fluorophore explores a slightly more hydrophilic environment in the phosphate/glycerol region (Mazeres et al., 1996).

Recently, ^{1}H magic angle spinning nuclear Overhauser enhancement spectroscopy (^{1}H MAS NOESY) has been applied quantitatively to investigate membrane structure

Received for publication 7 August 2000 and in final form 28 November 2000.

Address reprint requests to Dr. Andreas Herrmann, Humboldt-Universität zu Berlin, Mathematisch-Naturwissenschaftliche Fakultät I, Institut für Biologie/Biophysik, Invalidenstrasse 43, D-10115 Berlin, Germany. Tel.: 49-30-2093-8830; Fax: 49-30-2093-8585; E-mail: andreas=herrmann@rz.hu-berlin.de.

0006-3495/01/02/822/10 $2.00

and dynamics by measuring contact probabilities between lipid protons (Feller et al., 1999; Huster and Gawrisch, 1999; Huster et al., 1999). The ^{1}H MAS NOESY method is also very well suited to determine localization of small molecules such as ethanol (Holte and Gawrisch, 1997) or indole analogs (Yau et al., 1998) in the membrane. Typically, a broad distribution of these molecules in the bilayer rather than an exactly confined localization is found. This dynamic distribution profile is due to the fast motions of the molecules in the membrane resulting in the roughness of the membrane surface as revealed by x-ray measurements (Petrache et al., 1998; White and Wiener, 1996; Wiener and White, 1992).

Here, we report quantitative two-dimensional (2D) NOESY NMR data to assess the dynamical reorientation of the NBD moiety of C6-NBD-PC and C12-NBD-PC in 1-palmitoyl-2-oleoyl- *sn*-glycero-3-phosphocholine (POPC) vesicles. The quantitative analysis of cross-relaxation rates of NBD with lipid signals proves that the NBD group of both analogs is preferentially localized in the glycerol/upper chain region of the membrane, consistent with previous results by Chattopadhyay and London (1987). However, finite probabilities of contact between the NBD moiety and the bilayer center as well as the lipid headgroup, respectively, emphasize the dynamic properties of the probe and the width of the distribution range in the membrane. In membranes containing these NBD analogs, the order of chain segments localized in the lower, hydrophobic part is decreased. This is consistent with a looping back of the NBD-labeled chains to the lipid-water interface. The reorientation of the fluorescent moiety toward the aqueous environment was slightly more pronounced for the C12-NBD analog in comparison with C6-NBD-PC. In agreement with this observation we found a faster reduction of the NBD moiety by dithionite at the lipid-water interface for the C12-NBD analog in PC vesicles in comparison with the C6-NBD analog.

MATERIALS AND METHODS

Materials

1-Palmitoyl-2-[6-[(7-nitro-2–1,3-benzoxadiazol-4-yl)amino] caproyl]-*sn*-glycero-3-phosphocholine (C6-NBD-PC), 1-palmitoyl-2-[6-[(7-nitro-2–1,3-benzoxadiazol-4-yl)amino]dodecanoyl]-*sn*-glycero-3-phosphocholine (C12-NBD-PC), 1-palmitoyl-2-oleoyl-*sn*-glycero-3-phosphocholine (POPC), 1-palmitoyl-d_{31}-2-oleoyl-*sn*-glycero-3-phosphocholine (POPC-d_{31}), and egg yolk phosphatidylcholine (egg-PC) were purchased from Avanti Polar Lipids (Alabaster, AL) and Sigma (Deisenhofen, Germany), respectively, and used without further purification. The chemical structure of the two phospholipid analogs is depicted in Fig. 1.

Sample preparation

For NMR measurements, lipids were mixed in chloroform and evaporated under a stream of nitrogen. Subsequently, the lipid film was redissolved in approximately 500 μl of cyclohexan, frozen in liquid nitrogen, and lyophilized in a vacuum of less than 50 μbar resulting in a fluffy powder. Lipid powder was hydrated to 50 wt % with deuterium-depleted H_2O or D_2O for ^{2}H and ^{1}H NMR experiments, respectively. Lipid suspensions were vortexed, stirred and gently centrifuged for equilibration of the lipid water suspension. Then, lipid samples were transferred into 5-mm glass vials for static NMR experiments or 4-mm rotor inserts for MAS NMR experiments and sealed.

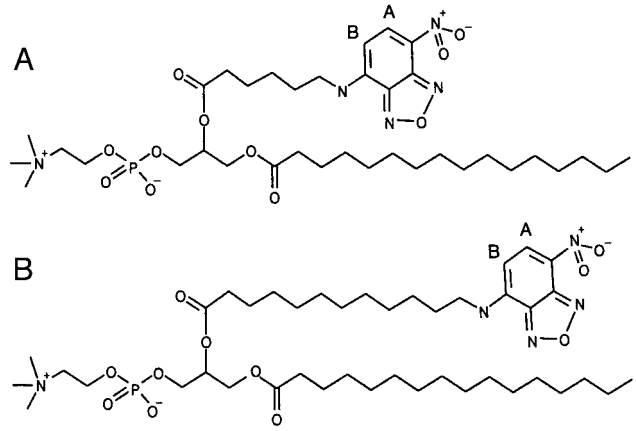

FIGURE 1 Chemical structure of the phospholipid analogs C6-NBD-PC (*a*) and C12-NBD-PC (*b*) used in this study. The protons on the ring system utilized for the magnetization exchange with lipid signals measured in the NOESY experiment are labeled A and B.

For fluorescence experiments, large unilamellar vesicles (LUVs) of egg-PC were symmetrically labeled with C6-NBD-PC or C12-NBD-PC; i.e., both membrane leaflets were labeled with the analogs. For that, lipids (egg-PC and NBD-lipids) dissolved in chloroform were combined in a glass tube and dried under nitrogen. Hepes-buffered saline (HBS, 150 mM NaCl, 10 mM Hepes, pH 7.4) was added to give a final lipid concentration of 4 mM (egg-PC) and 40 μM (NBD-lipids), respectively, and lipids were hydrated by vigorous vortexing followed by five freeze-thaw cycles for equilibration (Mayer et al., 1985). LUVs were prepared using the extrusion technique (extruder from Lipex Biomembranes, Vancouver, Canada) by filtration through 0.1-μm pores (10 cycles) at 40°C (Hope et al., 1985).

^{1}H MAS NMR

^{1}H MAS NMR experiments were carried out on a Bruker DRX600 spectrometer (Karlsruhe, Germany) at a resonance frequency of 600.13 MHz at a temperature of 30°C. The MAS spinning frequency was 10 kHz. Spectra were acquired at a spectral width of 6.7 kHz with a typical 90°-pulse length of 5.7 μs. Two-dimensional NOESY experiments (Wagner and Wüthrich, 1982; Jeener et al., 1979) were carried out with phase cycling in the States mode at mixing times of 1, 150, 300, and 450 ms. A total of 256 complex data points were collected in the indirect dimensions with 16 transients per increment at a relaxation delay of 4 s between successive scans. A square sine-bell window function was used in both dimensions before processing.

Peak volumes in 2D NOESY spectra were integrated using AURELIA software (Bruker Analytische Messtechnik, Rheinstaedten, Germany). NOE build-up curves were fitted to a spin pair model (Macura and Ernst, 1980) yielding cross-relaxation rates (σ_{ij}) according to

$$A_{ij}(t_m) = (A_{jj}(0)/2)(1 - \exp(-2\sigma_{ij}t_m))\exp(-t_m/T_{ij}). \quad (1)$$

The variable $A_{ij}(t_m)$ represents the cross-peak volume at mixing time t_m and $A_{jj}(0)$ the diagonal peak volume at mixing time 0. The value $1/T_{ij}$ defines a rate of magnetization leakage toward the lattice. Cross-relaxation rates were obtained from fits of experimental cross-peak volumes at varying

mixing times to Eq. 1 using the nonlinear regression curve fitter in SigmaPlot (Jandel Scientific Software, San Rafael, CA).

^{2}H and ^{31}P solid-state NMR

^{31}P NMR spectra were accumulated on a Bruker DSX400 NMR spectrometer operating at 162.12 MHz using a high-power probe equipped with a 5-mm solenoid sample coil. A Hahn-echo pulse sequence with a 90°-pulse length of 5 μs, a 50-μs delay between pulses, a spectral width of 125 kHz, and a relaxation delay of 1 s was used. Broadband proton decoupling was applied during the pulse and acquisition periods.

^{2}H NMR spectra were also recorded on a Bruker DSX400 NMR spectrometer at a resonance frequency of 61.48 MHz. Spectra were accumulated applying a phase-cycled quadrupolar echo pulse sequence (Davis et al., 1976) using 3.5-μs 90° pulses separated by a 50-μs delay, a spectral width of 200 kHz, and a recycle delay of 0.4 s. All solid-state NMR measurements were carried out at a temperature of 30°C.

^{2}H NMR powder spectra were de-Paked (Sternin et al., 1983) using the algorithm of McCabe and Wassall (1995) as described in detail in Huster et al. (1998). Smoothed order parameter profiles (Lafleur et al., 1989) were determined from the quadrupolar splittings ($\Delta\nu_Q$) according to

$$\Delta\nu_Q = \frac{3}{4}\frac{e^2qQ}{h}S(n), \qquad (2)$$

where e^2qQ/h is the quadrupolar coupling constant (167 kHz for deuterons in the C—^{2}H bond) and $S(n)$ the chain order parameter for carbon number n.

Dithionite assay and fluorescence measurements

Dithionite destroys the NBD fluorescence by chemical reduction of the respective NO group (McIntyre and Sleight, 1991). The dithionite-mediated decrease of NBD fluorescence of LUVs symmetrically labeled with C6-NBD-PC or C12-NBD-PC was followed. Fifty microliters of labeled LUVs were diluted in 2 ml of HBS, and fluorescence intensity was monitored at 25°C (see inset of Fig. 7). After 30 s, dithionite was added (left arrow in the inset of Fig. 7) from an ice-cold 1 M stock solution in 100 mM Tris, pH 10, to give various final concentrations. At the end of each measurement Triton X-100 was added (final concentration 0.5% (v/v)) to allow the reduction of all analogs (see right arrow in the inset of Fig. 7). Fluorescence was measured at an Aminco Bowman spectrometer series 2 (Rochester, NY) with an excitation and emission wave length of 470 and 540 nm, respectively, and slit widths of 4 nm. After subtraction of the baseline, curves were normalized to the fluorescence intensity in the absence of dithionite (mean fluorescence intensity in the first 30 s; see Fig. 7).

At dithionite concentrations above 100 mM, the reduction of fluorescence was too rapid to be resolved with this method (see inset of Fig. 7). Therefore, we followed the decrease of fluorescence at higher dithionite concentrations using a stopped-flow equipment (RX 1000 Rapid Kinetics from Applied Photophysics, Surrey, UK) connected to the fluorescence spectrometer. The two chambers of the stopped-flow device were filled with the solution of labeled LUVs (100 μM egg-PC, 1 μM NBD-PL) and with the dithionite solution having different concentrations. After mixing both solutions, fluorescence was followed at 540 nm (excitation 470 nm, slit width each 4 nm) with a time resolution of 0.1 s at 25°C. The dead time of the stopped-flow apparatus is 10 ms. Five to ten single measurements under identical conditions were accumulated for improving the signal-to-noise ratio. The curves of fluorescence decay were fitted to the sum of two exponentials (see Results) using the software SigmaPlot.

RESULTS

^{31}P and ^{2}H NMR

Fig. 2 shows ^{31}P and ^{2}H NMR spectra of POPC-d_{31} in the absence and presence of NBD analogs incorporated at a molar ratio of 3:1. The motionally averaged axially symmetric ^{31}P shielding tensors are indicative of a lamellar liquid crystalline membrane phase both in the presence (Fig. 2, *b* and *c*) and absence (Fig. 2 *a*) of the NBD analogs. The chemical shift anisotropy $\Delta\sigma$ has been obtained from line shape simulation of the ^{31}P powder patterns (dashed lines). In the presence of NBD-PC, $\Delta\sigma$ decreases slightly from $\Delta\sigma$ = 45.8 ppm for pure POPC membranes to $\Delta\sigma$ = 44.1 ppm for C6-NBD-PC and $\Delta\sigma$ = 43.7 ppm for C12-NBD-PC, respectively. An exponential line broadening of 1.5, 2.8, and 2.9 ppm was used in the simulation of spectra *a*, *b*, and *c*, respectively. For spectrum *b*, a slight orientation in the magnetic field was assumed for the simulation modeled by an ellipsoidal distribution with an axis ratio of 0.9 to 1.

^{2}H NMR spectra of chain-deuterated POPC-d_{31} in the absence (Fig. 2 *d*) and presence of C6-NBC-PC (Fig. 2 *e*) and C12-NBD-PC (Fig. 2 *f*) are shown in the right column of Fig. 2. The presence of the NBD analogs affects the width of the quadrupolar splittings. Although the larger quadrupolar splittings are only weakly reduced, a more pronounced reduction of the narrow quadrupolar splittings

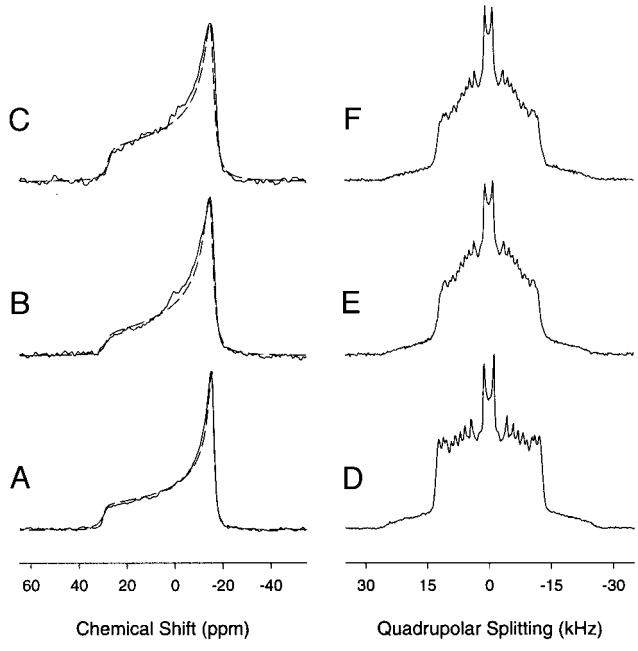

FIGURE 2 ^{31}P (*left column*) and ^{2}H (*right column*) spectra of POPC-d_{31} in the absence (*a* and *d*) and in the presence of C6-NBD-PC (*b* and *e*) and C12-NBD-PC (*c* and *f*) at 50 wt % H_2O and a temperature of 30°C. The molar ratio of NBD analogs and POPC was 1:3. Dashed lines represent line shape simulation for the ^{31}P powder patterns using a chemical shift anisotropy of $\Delta\sigma$ = 45.8 ppm (*a*), $\Delta\sigma$ = 44.1 ppm (*b*), and $\Delta\sigma$ = 43.7 ppm (*c*).

that correspond to the terminal methylene groups of the lipid chains is observed.

To quantify these changes along the hydrophobic chains, smoothed chain order parameter profiles (Lafleur et al., 1989) and difference order parameter plots (Nezil and Bloom, 1992) are generated (Fig. 3). Order parameter profile analysis reveals NBD induced changes of lipid chain order. Lipid chain order of POPC is decreased in the presence of both lipid analogs. The order decrease is more pronounced for middle and lower chain segments whereas upper chain segments experience only a moderate order decrease (Fig. 3 *b*). Such order changes are consistent with a preferential localization of the NBD moiety at the lipid-water interface. Interface location of the NBD group provides lower and middle chain segments with more motional freedom than the upper chain and correspondingly decreases molecular order (see Discussion).

Quantitative ^{1}H MAS NOESY cross-peak analysis

In Fig. 4, the ^{1}H MAS spectrum of a 3:1 (mol/mol) mixture of POPC and C6-NBD-PC at a spinning speed of 10 kHz is depicted. The assignment of the pure phospholipid spectrum is found in literature (Forbes et al., 1988b; Volke and Pampel, 1995). As shown by a double quantum filtered COSY experiment (Rance et al., 1983) in chloroform solution under high-resolution NMR conditions, the methylene group in the short chain next to the nitrogen (see Fig. 1) is superimposed with the signal of the CH_2-N of the phospholipid headgroup (β protons at 3.7 ppm). The other methylene signals of the short fatty acid chain appear slightly downfield shifted from most of the chain methylene signals. The two proton signals of NBD were assigned according to the reference of pure NBD provided in the Integrated Spectral Data Base System for Organic Compounds (http://www.aist.go.jp/RIODB/SDBS/). The signal of proton B of the NBD ring system (see Fig. 1) is rather narrow whereas proton A exhibits some broadening. The origin of this broadening is unknown at the moment but could be related to the vicinity of the charged dipole on the ring system.

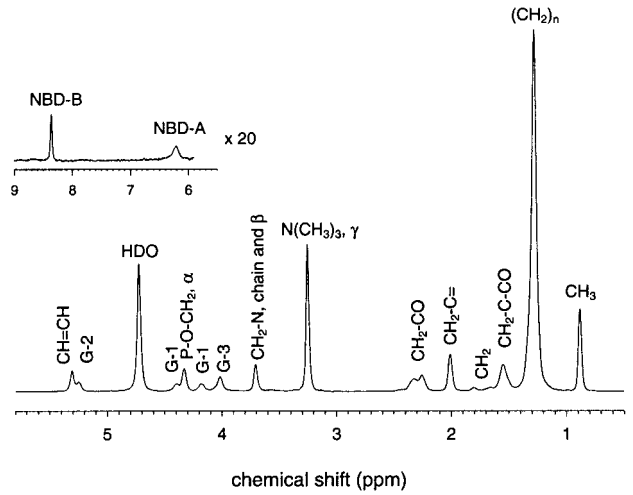

FIGURE 4 600 MHz ^{1}H MAS spectrum of C6-NBD-PC in a POPC phospholipid matrix at 50 wt % D_2O at a spinning speed of 10 kHz and a temperature of 30°C.The inset shows the downfield region of the spectrum with the proton signals from the NBD ring system at a 20-fold amplification. The molar ratio of NBD analogs and POPC was 1:3.

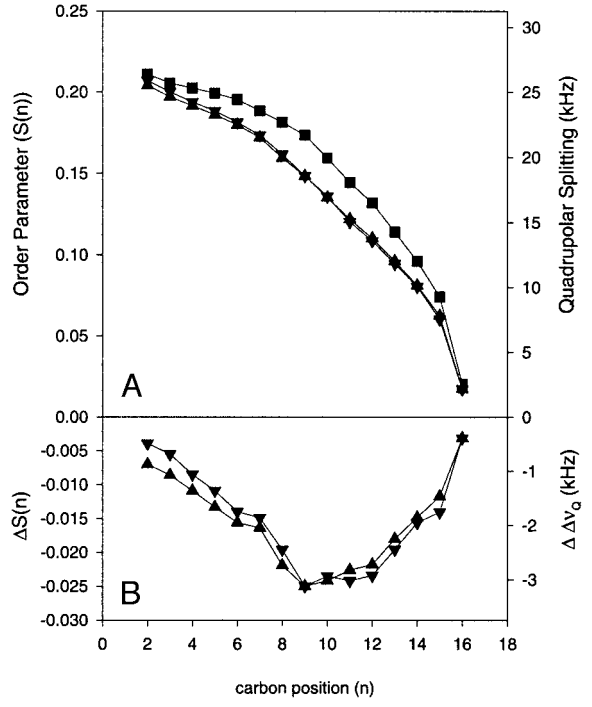

FIGURE 3 Order parameter profiles (*a*) and difference order parameter plots (*b*) for the ^{2}H NMR spectra at 30°C shown in Fig. 2. Order parameter profiles are shown for POPC-d_{31} in the absence (■]), and in the presence of 25 mol % C6-NBD-PC (▲) and C12-NBD-PC (▼). Difference order parameter plots are obtained by subtraction of the order parameter profile of POPC-d_{31} in the absence of the NBD analog from the profile calculated in the presence of C6-NBD-PC (▲) and C12-NBD-PC (▼), respectively.

In Fig. 5 a contour plot of the NBD-B region of the 2D NOESY spectrum of C12-NBD-PC/POPC (1:3, mol/mol) at a mixing time of 300 ms is plotted showing the cross-peaks of the B signal of the NBD ring with all other lipid signals. As demonstrated previously, lipid-lipid cross-peaks are of intermolecular origin except for directly neighboring methylene groups (Huster et al., 1999). Furthermore, a very strong intramolecular cross-peak between the NBD-B and NBD-A signals is present. Intermolecular NBD-lipid cross-peaks with all other resolved peaks in the spectrum are found covering the entire range from the hydrophobic terminus of the phospholipid chains to the headgroup protons. Intensity differences between the cross-peaks are due to varying number of protons contributing to the magnetization exchange as well as differences in the contact probability between those protons. Therefore, only a quantitative

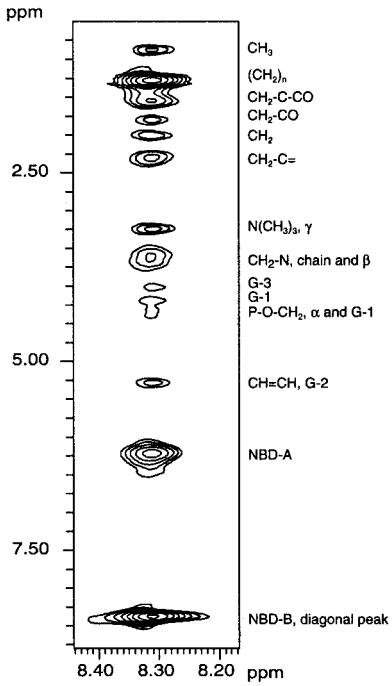

FIGURE 5 Contour plot of the NBD-B region of a ^{1}H MAS NOESY spectrum at a mixing time of 300 ms showing the cross-peaks of the NBD-B proton with all other lipid signals. Data were recorded in a phase-sensitive mode. All cross-peaks have positive intensity. A total of 16 transients per t_1 increment have been accumulated, yielding in a total acquisition time of approximately 5 h. The molar ratio of NBD analogs and POPC was 1:3.

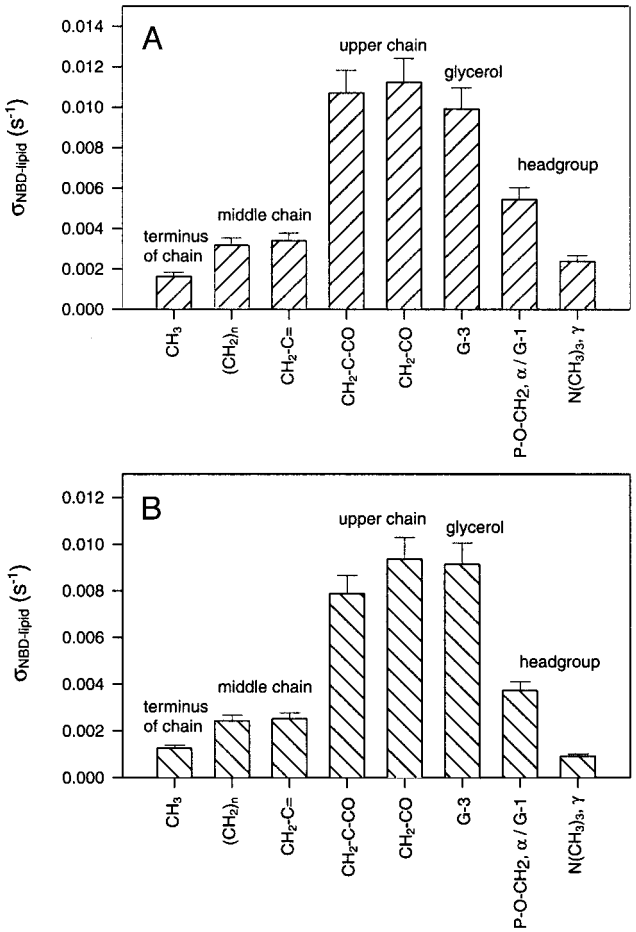

FIGURE 6 Cross-relaxation rates (s^{-1}) between the B proton of the NBD ring system (see Fig. 5 for assignment) and protons of phospholipid analogs for C6-NBD-PC (*a*) and C12-NBD-PC (*b*) in mixture with POPC (1:3, mol/mol). Cross-relaxation rates represent the contact probability for the B proton of the NBD group with the respective protons of POPC (Huster et al., 1999). Cross-relaxation rates were calculated using the two-spin exchange model (Macura and Ernst, 1980) according to Eq. 1.

analysis of cross-relaxation rates provides insights into localization of the NBD group in the lipid bilayer.

The NOESY cross-peaks were integrated and cross-relaxation rates determined according to Eq. 1. Cross-peak volumes can be well fitted with the spin pair exchange model. The reproducibility of cross-relaxation rate determination between independent experiments is typically around $\pm$10–15% (Huster and Gawrisch, 1999); therefore, a rather accurate value for the cross-relaxation rates can be provided. Absolute cross-relaxation rates for contacts between the NBD ring and various phospholipid protons are plotted in Fig. 6 for both NBD analogs. All cross-relaxation rates for C12-NBD-PC are approximately 10% smaller compared with C6-NBD-PC, which presumably indicates a slightly different mixing ratio in the two preparations. Cross-relaxation rates reflect the probability of contacts between protons. Highest probability for NBD-lipid contacts is found for both the upper part of the fatty acid chain and glycerol region, a region that is commonly referred to as the lipid-water interface. Significantly smaller probabilities are found for contacts between NBD group and the middle part and, even smaller, the terminus of the chains. Similarly, contact probability decreases toward the lipid headgroup.

Although within the experimental error, small differences of the contact probability profiles are detected between the two NBD analogs. For C12-NBD-PC, contact probability for the upper part of the chain is somewhat reduced whereas a higher contact probability with the glycerol is observed (Fig. 6 *b*). On the other hand, the contact probability with the headgroup is somewhat smaller. From the NMR data, a distribution of the NBD group localization in the lipid bilayer can be concluded with a pronounced preference at the upper chain/glycerol region.

Fluorescence measurements

To obtain independent evidence for the localization of the NBD moiety, we have measured the dithionite-mediated reduction of the NBD group of C6-NBD-PC and C12-NBD-PC, respectively, in egg-PC-LUVs. Upon addition of dithionite at various concentrations (up to 200 mM) to the cuvette containing labeled LUVs, we observed a rapid drop of the

fluorescence intensity to ~50% of the initial value (Fig. 7, *inset*, shown only for C12-NBD-PC at 10 and 100 mM dithionite). This fluorescence decrease is caused by the irreversible reaction of dithionite with the NBD analogs localized on the outer leaflet, i.e., the leaflet exposed to dithionite. The rapid decline was followed by a very slow phase of fluorescence loss. Very likely, this corresponds to reduction of analogs on the inner leaflet subsequent to permeation of dithionite. It is already known that dithionite permeates lipid bilayers only very slowly (McIntyre and Sleight, 1991). After solubilization of LUVs by addition of Trition X-100 all analogs on the inner leaflet became immediately accessible to dithionite (Fig. 7, *inset, right arrow*).

Cuvette experiments do not allow resolving appropriately the initial phase of the fluorescence decrease at dithionite concentration ≥100 mM (see Fig. 7, *inset, curve D*). In those experiments mixing time is of the order of only ~1 s. Therefore, we employed a stopped-flow technique to follow the decrease of fluorescence in the presence of dithionite at ≥100 mM. For example, the kinetics of fluorescence decrease of C6-NBD-PC and C12-NBD-PC upon mixing with 100 mM dithionite is shown in Fig. 7. Similar to the cuvette experiments carried out in parallel, we found a rapid drop of the fluorescence intensity by ~50% consistent with the complete reduction of analogs in the outer leaflet.

The initial rapid decrease of fluorescence upon addition of dithionite was faster for C12-NBD-PC compared with C6-NBD-PC (shown for 100 mM dithionite; compare *curves B* and *A*, Fig. 7). This difference was observed over the entire concentration range of dithionite employed. To quantify the kinetics, experimental curves were fitted to two exponentials. The rate constant k_1 corresponds to the reaction of dithionite with analogs on the outer leaflet, which can be considered as pseudo-monoexponential. Permeation of dithionite and its reaction with analogs on the inner leaflet were lumped into the rate constant k_2. Although the two monoexponentials fit the experimental curves well (see Fig. 7) we are aware that this treatment is an oversimplification. However, our main goal was to determine k_1.

The values for k_1 in dependence on dithionite concentration are shown in Fig. 8. It can be seen that k_1 depends on the dithionite concentration reaching a plateau value at ~200 mM dithionite (Fig. 8). Independent of the dithionite concentration we found a higher rate constant k_1 for C12-NBD-PC in comparison with C6-NBD-PC; e.g., at 200 mM dithionite, k_1 of C12-NBD-PC was ~1.4 times of that of C6-NBD-PC. As expected, the rate constant k_2 (data not shown) is at least more than one order of magnitude lower in comparison with k_1 for both analogs. Above 10 mM dithionite, the difference is even more pronounced, amounting to more than two orders of magnitude. By that observation and the similar order parameter profiles of both analogs (see above), we can conclude that the reduction of NBD is not affected by an analog-dependent perturbation of the lipid bilayer organization giving rise to the faster reduction of C12-NBD-PC by dithionite. From these results, we conclude that compared with C6-NBD-PC, the NBD group

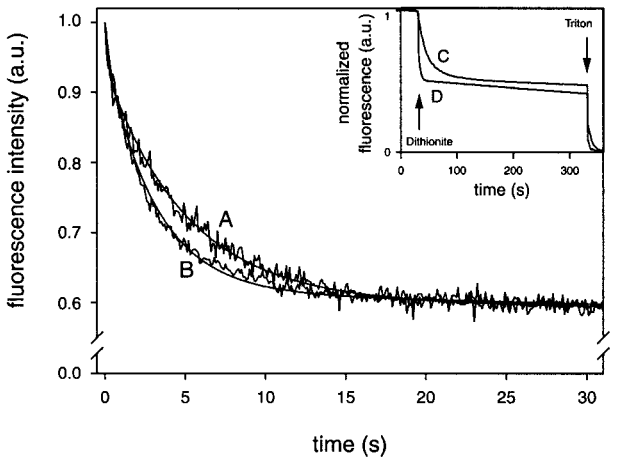

FIGURE 7 Reduction of NBD-labeled analogs in egg-PC liposomes by dithionite at 25°C. Reduction of the fluorescence intensity of C6-NBD-PC (*curve A*) and C12-NBD-PC (*curve B*) was measured in the presence of 100 mM dithionite employing a stopped-flow device as described in Materials and Methods. At time $t = 0$, mixing was started. Curves are the average of five single measurements. Kinetics are fitted to the sum of two exponentials (see Materials and Methods and Results). (*Inset*) Reduction of C12-NBD-PC was measured in a cuvette experiment (see Materials and Methods and Results); 10 mM (*curve C*) or 100 mM (*curve D*) dithionite were added (*left arrow*) and the fluorescence intensity was measured. Subsequently, analogs on the inner leaflet were made accessible to dithionite by solubilization of vesicles by Triton X-100 (0.5%) (*right arrow*).

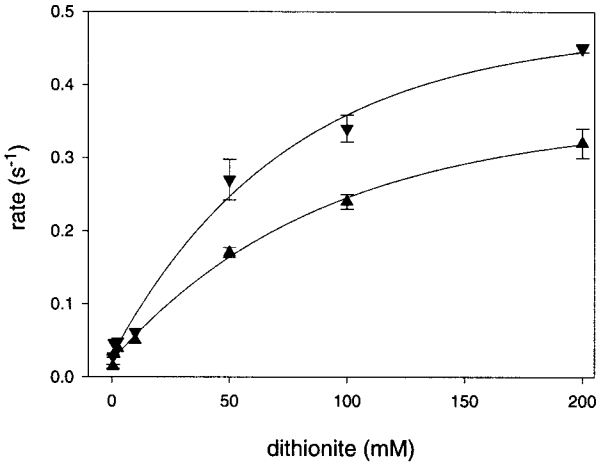

FIGURE 8 Reduction of the NBD moiety of analogs on the outer leaflet of egg-PC vesicles as a function of the dithionite concentration. Kinetics of cuvette experiments (≤50 mM) and stopped-flow measurements (≥100 mM) were fitted to the sum of two exponentials (see Materials and Methods and Results). The rate constant k_1 reflecting the kinetics of reduction of analogs on the outer leaflet is shown for C6-NBD-PC (▲) and C12-NBD-PC (▼). Data of three to five independent measurements are shown (average ± standard error of estimate). Data were fitted as described in Materials and Methods and Results.

of C12-NBD-PC is more strongly exposed to the polar interface and, therefore, reacting more efficiently with the polar dithionite.

DISCUSSION

Localization of the covalently attached NBD ring system in the lipid-water interface

The three methods employed in this study reveal 1) a highly dynamic reorientation of the *sn2*-chain-attached NBD group parallel to the membrane normal and 2) a preferential localization of NBD in the lipid-water interface, which 3) is more pronounced for the C12-NBD-PC analog.

A small decrease in the ^{31}P chemical shift anisotropy of the PC headgroup is observed in the presence of both NBD analogs. This indicates a change in the chemical environment of the lipid phosphate groups consistent with the looping back of the NBD group. The change in the phosphorous chemical shift anisotropy is somewhat larger for the long-chain analog, but this difference is within experimental error of ± 1 ppm.

The ^{2}H NMR order parameter analysis provides a qualitative measure of the NBD localization. The ring system placed in the glycerol/upper chain region of the lipid membrane acts as a spacer between neighboring lipid molecules providing lower lipid chain segments with more motional freedom. As a result, a decrease of molecular order for the lower part of the chain is detected. Similar changes in ^{2}H NMR order parameters have been reported for small molecules located in the lipid water interface of a membrane such as ethanol (Barry and Gawrisch, 1995) or indole analogs (Yau et al., 1998). Typically, similar order changes are obtained at higher loadings for ethanol or indole analogs (molar ratios in these studies were between 0.6 and 0.9). Therefore, we conclude that the upturning acyl chain of NBD-PC analogs may contribute to the disordering of the lipid matrix.

Converting changes of lipid chain order into area per molecule changes (Seelig and Seelig, 1974; Nagle, 1993), the NBD induced lipid chain disordering corresponds to an increase in average area per POPC molecule of approximately 2.0 and 1.9 Å^2 for C6-NBD-PC and C12-NBD-PC, respectively. Assuming an average cross-sectional area per POPC molecule of 62 Å^2 in the bilayer (Pabst et al., 2000), these changes represent an $\sim$3% increase of the area per molecule.

A more quantitative picture of the NBD localization is provided by the ^{1}H MAS NOESY measurement. It has been established that NOESY cross-relaxation rates in lipids report intermolecular contact probabilities between molecular segments (Huster and Gawrisch, 1999; Huster et al., 1999). Initially, this appeared surprising in consideration of the multitude of lipid motions on time scales covering several orders of magnitude. However, as shown by a combined NMR and molecular dynamics simulation study (Yau and Gawrisch, 2000; Feller et al., 1999), only the rather slow motions of the entire lipid molecule significantly contribute to cross-relaxation, i.e., the lateral diffusion of lipid molecules with a correlation time for a two-site exchange of 170 ns (Pastor and Feller, 1996). Due to the covalent attachment to the lipid chain, it is reasonable to assume that the NBD moiety also experiences this motion. Therefore, a similar correlation time is likely to modulate cross-relaxation between NBD and lipid segments although smaller molecules in the lipid-water interface may perform faster motions that modulate the NOE (Holte and Gawrisch, 1997).

The influence of spin diffusion as an alternative mechanism for magnetization transfer compared with direct contacts has been discussed in several papers (Chen and Stark, 1996; Forbes et al., 1988a). Typically, ^{1}H-^{1}H cross-relaxation rates in monounsaturated lipids are much smaller than 1 s^{-1} (Yau and Gawrisch, 2000), which indicates that spin diffusion can be neglected at mixing times of a few hundred milliseconds. Furthermore, as shown recently, cross-relaxation rates in specifically deuterated lipid membranes where spin diffusion is blocked by deuteration are indistinguishable from nondeuterated samples, proving that spin diffusion does not contribute significantly to magnetization exchange up to mixing times of the order of 500 ms (Huster and Gawrisch, 1999).

Protons of the NBD group exchange magnetization with all lipid protons (Figs. 5 and 6). Despite the dynamical reorientation of the NBD group, a clear maximum of the contact probabilities is obtained for magnetization exchange with the glycerol/upper chain segments, suggesting a preferential localization in that region. Furthermore, finite contact probabilities of NBD protons with protons of the hydrophobic chain terminus as well as of the lipid headgroup are obtained emphasizing again the dynamical reorientation of the probe around the localization of lowest free energy. The distribution of the contact probability obtained for NBD is in qualitative agreement with the profiles obtained for other interface-located molecules such as ethanol and indole (Yau et al., 1998; Holte and Gawrisch, 1997).

From differences of the cross-relaxation profiles between the two NBD analogs we surmise for C12-NBD-PC a position of the NBD group slightly closer to the aqueous phase in comparison with that of C6-NBD-PC. Although within experimental error, cross-relaxation rates of the upper chain with NBD decrease and those of the glycerol with NBD increase slightly for C12-NBD-PC compared with C6-NBD-PC. Indeed, support for this result is given by the accessibility of dithionite to the NBD groups. The more efficient destruction of the NBD fluorescence for C12-NBD-PC strongly suggests a better accessibility for this analog by dithionite. Because dithionite permeates lipid membranes only very slowly (McIntyre and Sleight, 1991) it can be concluded that the more efficient reaction of dithionite with C12-NBD-PC is due to a localization of the

probe closer to the aqueous environment. Of course, this approach does not allow determination of the dynamical reorientation of the NBD group as provided by the NMR techniques applied here.

Some uncertainties may arise from the different NBD analog concentrations applied in NMR and fluorescence measurements. For sensitivity reasons, NMR measurements have to be carried out at much higher loads of NBD analogs in the membrane. However, because both NMR and fluorescence report the looping back of the acyl chains and the NBD location in the lipid water interface it is unlikely that the high analog concentration used in the NMR measurements influences its location in the lipid water interface of the bilayer.

The localization of the fatty-acid-attached NBD group of lipid analogs revealed by our study agrees with previous results by Chattopadhyay and London (1987). Nevertheless, the localization of the fluorescence probe determined by a fluorescence-quenching assay represents an average over at least several angstroms due to the distribution depths of fluorophores and spin labels (Chattopadhyay and London, 1987). In contrast, our NOESY NMR data provide a quantitative picture of the dynamic width of the NBD distribution profile, which extends over the entire width of a membrane leaflet. They are also in agreement with the proposed looping back of the NBD group to the lipid-water interface (Chattopadhyay and London, 1987). This looping back is considered as a serious disadvantage for employing those analogs as reporters of the endogenous lipids. For the latter, a reorientation of the hydrophobic chains toward the polar interface of the membrane has been regarded as rather atypical. However, very recently it has been shown by 2D MAS NOESY NMR that due to the high degree of motional disorder in phospholipid membranes direct contacts of the hydrocarbon chains with the headgroups are significant (Huster and Gawrisch, 1999; 2000; Huster et al., 1999). This implies that looping back of flexible acyl chains with an attached NBD group may not be in qualitative contrast to the behavior of unlabeled chains. Nevertheless, the distribution profile of the terminal CH_3 group of a phospholipid chain has its maximum at lower and middle chain segments whereas contacts with upper chain, glycerol, and headgroup segments have a significantly smaller probability (Yau and Gawrisch, 2000; Huster et al., 1999). Although molecular disorder due to thermal energy is responsible for the occasional phospholipid chain upturns, the orientation of the NBD ring system toward the lipid-water interface is driven by other forces (see below).

Thus, our study underlines that conclusions from the behavior of those NBD-labeled phospholipid analogs for the organization and dynamics of respective endogenous phospholipids have to be drawn with caution for the following reasons: 1) the presence of an artificial (NBD) moiety, 2) the localization of this moiety in the membrane due to the looping back behavior, and 3) the accompanied perturbation of lipid chain order. In particular, the NBD group may significantly influence the affinity to membrane proteins, e.g., to lipid translocators. Furthermore, due to its localization in the lipid-water interface, the NBD moiety is sensitive to properties of this interface and their alterations. For instance, changes of the surface potential may effect the position of the NBD group perpendicular to the membrane surface. Although this would recommend the use of those analogs for detecting interface properties (see below), changes of the localization of the NBD group may affect the affinity of analogs to membrane proteins not relevant for endogenous lipids. As already mentioned, analogs with a longer fatty acid chain in the *sn2*-position such as the C12-NBD-PC are considered to better reflect the behavior of endogenous lipids than those with a short fatty acid chain. From our study, we can add that this is not related to a diminished looping back of the NBD moiety of analogs with a longer fatty acid chain compared with those of a shorter chain. Rather, we suggest that the preference in choosing C12-NBD-analogs over C6-NBD-analogs may arise from a deeper insertion of the *sn2*-fatty acid chain and its loop into the hydrophobic part of the membrane resulting in a more stable insertion. Eventually, being aware of the structural limitations, the use of those analogs has been shown to contribute significantly to understanding of transbilayer dynamics and of intracellular trafficking of lipids.

What interactions determine the preferential localization of the NBD ring system in the lipid-water interface?

A number of factors have to be considered when the physical background for the experimentally determined localization of the NBD group is explored. First of all, aromatic compounds exhibit a high propensity toward a hydrophobic environment due to the hydrophobic effect. However, this mechanism would account for NBD localization in the membrane core rather than in the interface. Therefore, specificities of the NBD ring system as well as of the fluid bilayer milieu have to be taken into account.

NBD is an aromatic molecule that carries localized charges as well as a dipole moment arising from both the fixed charge distribution and the asymmetry in electron density over the ring system. On the other hand, the phospholipid surface/interface exhibits a complex electrostatic environment with fixed charges due to the phosphate and choline groups as well as dipole moments arising from the carbonyl groups of the upper chains, the water molecules, and the PC headgroup dipole (Gawrisch et al., 1992). Therefore, a variety of favorable Coulombic, dipole-charge, and dipole-dipole interactions may decrease the free energy of the NBD ring if located in the membrane interface.

An additional electrostatic interaction that has to be considered is the cation-π electron interaction between the positively charged choline and the NBD group of the lipid.

The aromatic ring system of NBD gives rise to an electric quadrupole moment that interacts with positive charges. These cation-π electron interactions are a relevant factor in determination of biological structures and their dynamics (Dougherty, 1996).

Hydrogen bonds represent a further favorable interaction of the NBD group in the lipid-water interface. The imino group and the oxygens of the NBD probe may form hydrogen bonds with the lipid carbonyls, water molecules, and the lipid headgroup. Finally, lipid-induced contributions to the minimum of free energy have to be considered as lipid chains undergo a disordering due to the interface localization of NBD, which increases chain entropy.

At the moment, no quantitative estimate can be given for the individual contribution of the various interactions. Most likely, the polar NO_2 group will be that part of the NBD moiety that will orient most strongly toward the aqueous phase whereas the part linked to the lipid chain will point toward the membrane interior. The interface localization may then be determined by a force equilibrium between the hydrophobic interactions dragging the ring system deeper into the membrane core and the electrostatic interactions and hydrogen bonding of NBD with the lipid headgroup, the carbonyl, and water molecules pushing the NBD group to the lipid-water interface. However, a remarkable observation of our study is that the looping back of the NBD group is not reduced for the C12-NBD-PC analog compared with C6-NBD-PC. On the contrary, in particular the dithionite assay suggests a stronger exposure of the NBD group of C12-NBD-PC to the lipid-water interface. We hypothesize that this might be due to the longer C12 chain providing a flexibility that allows the NBD group to extend farther into the aqueous phase.

The lipid-water interface of phospholipid membranes also hosts other aromatic compounds such as amino acid side chains and indole analogs (Wimley and White, 1993; Yau et al., 1998; Persson et al., 1998), emphasizing the importance of that region for protein membrane interactions (White and Wimley, 1999). The membrane thickness and structural complexity of the lipid-water interface of a membrane is due to the constantly fluctuating lipid molecules performing a large variety of reorientations on a time scale from micro- to picoseconds (Huster et al., 1999; Pastor and Feller, 1996; Wiener and White, 1992). The localization of the chain-attached NBD ring system in the lipid-water interface makes it a useful probe for investigation of phenomena occurring in that region. However, the motional freedom and fast thermal fluctuations of the probe must be considered.

We thank Prof. Mei Hong (Iowa State University, Ames, IA) for making the DSX400 spectrometer available for solid-state NMR measurements, Dr. Matthias Jank (University of Leipzig) for providing access to the AURELIA software, and Mrs. Bärbel Hillebrecht (Humboldt-University) for her assistance in doing fluorescence measurements. We are indebted to Prof. P. Devaux (Institut de Biologie-Physico Chimique, Paris) for critical reading of the manuscript and helpful comments.

The work was supported by the Deutsche Forschungsgemeinschaft (SFB197 to K.A., He1928 to A.H., and Mu1017 to P.M.). Part of the study was carried out while D.H. received a postdoctoral fellowship from the BASF AG through the Studienstiftung des deutschen Volkes.

REFERENCES

Barry, J. A., and K. Gawrisch. 1995. Effects of ethanol on lipid bilayers containing cholesterol, gangliosides, and sphingomyelin. *Biochemistry.* 34:8852–8860.

Chattopadhyay, A., and E. London. 1987. Parallax method for direct measurement of membrane penetration depth utilizing fluorescence quenching by spin-labeled phospholipids. *Biochemistry.* 26:39–45.

Chen, Z. J., and R. E. Stark. 1996. Evaluating spin diffusion in MAS-NOESY spectra of phospholipid multibilayers. *Solid State Nucl. Magn. Reson.* 7:239–246.

Colleau, M., P. Herve, P. Fellmann, and P. F. Devaux. 1991. Transmembrane diffusion of fluorescent phospholipids in human erythrocytes. *Chem. Phys. Lipids.* 57:29–37.

Comfurius, P., J. M. Senden, R. H. Tilly, A. J. Schroit, E. M. Bevers, and R. F. Zwaal. 1990. Loss of membrane phospholipid asymmetry in platelets and red cells may be associated with calcium-induced shedding of plasma membrane and inhibition of aminophospholipid translocase. *Biochim. Biophys. Acta.* 1026:153–160.

Connor, J., K. Gillum, and A. J. Schroit. 1990. Maintenance of lipid asymmetry in red blood cells and ghosts: effect of divalent cations and serum albumin on the transbilayer distribution of phosphatidylserine. *Biochim. Biophys. Acta.* 1025:82–86.

Connor, J., C. C. Pak, and A. J. Schroit. 1994. Exposure of phosphatidylserine in the outer leaflet of human red blood cells. Relationship to cell density, cell age, and clearance by mononuclear cells. *J. Biol. Chem.* 269:2399–2404.

Davis, J. H., K. R. Jeffrey, M. Bloom, M. I. Valic, and T. P. Higgs. 1976. Quadrupolar echo deuteron magnetic resonance spectroscopy in ordered hydrocarbon chains. *Chem. Phys. Lett.* 42:390–394.

Dougherty, D. A. 1996. Cation-pi interactions in chemistry and biology: a new view of benzene, Phe, Tyr, and Trp. *Science.* 271:163–168.

Feller, S. E., D. Huster, and K. Gawrisch. 1999. Interpretation of NOESY cross-relaxation rates from molecular dynamics simulations of a lipid bilayer. *J. Am. Chem. Soc.* 121:8963–8964.

Forbes, J., J. Bowers, X. Shan, L. Moran, E. Oldfield, and M. A. Moscarello. 1988a. Some new developments in solid-state nuclear magnetic resonance spectroscopic studies of lipids and biological membranes, including the effect of cholesterol in model and natural systems. *J. Chem. Soc. Faraday Trans.* 184:3821–3849.

Forbes, J., C. Husted, and E. Oldfield. 1988b. High-field, high-resolution proton "magic-angle" sample-spinning nuclear magnetic resonance spectroscopic studies of gel and liquid crystalline lipid bilayers and the effects of cholesterol. *J. Am. Chem. Soc.* 110:1059–1065.

Gawrisch, K., D. Ruston, J. Zimmerberg, V. A. Parsegian, R. P. Rand, and N. Fuller. 1992. Membrane dipole potentials, hydration forces, and the ordering of water at membrane surfaces. *Biophys. J.* 61:1213–1223.

Holte, L. L., and K. Gawrisch. 1997. Determining ethanol distribution in phospholipid multilayers with MAS-NOESY spectra. *Biochemistry.* 36: 4669–4674.

Hope, M. J., M. B. Bally, G. Webb, and P. R. Cullis. 1985. Production of large unilamellar vesicles by a rapid extrusion procedure. Characterization of size distribution, trapped volume, and ability to maintain a membrane potential. *Biochim. Biophys. Acta.* 812:55–65.

Hrafnsdottir, S., J. W. Nichols, and A. K. Menon. 1997. Transbilayer movement of fluorescent phospholipids in *Bacillus megaterium* membrane vesicles. *Biochemistry.* 36:4969–4978.

Huster, D., K. Arnold, and K. Gawrisch. 1998. Influence of docosahexaenoic acid and cholesterol on lateral lipid organization in phospholipid membranes. *Biochemistry.* 37:17299–17308.

Huster, D., K. Arnold, and K. Gawrisch. 1999. Investigation of lipid organization in biological membranes by two-dimensional nuclear Overhauser enhancement spectroscopy. *J. Phys. Chem. B.* 103:243–251.

Huster, D., and K. Gawrisch. 1999. NOESY NMR crosspeaks between lipid headgroups and hydrocarbon chains: spin diffusion or molecular disorder? *J. Am. Chem. Soc.* 121:1992–1993.

Huster, D., and K. Gawrisch. 2000. New insights into biomembrane structure from two-dimensional nuclear Overhauser enhancement spectroscopy. *In* Lipid Bilayers: Structure and Interactions. J. Katsaras and T. Gutberlet, editors. Springer-Verlag, Berlin. 109–125.

Jeener, J., B. H. Meier, P. Bachmann, and R. R. Ernst. 1979. Investigation of exchange processes by two-dimensional NMR spectroscopy. *J. Chem. Phys.* 71:4546–4553.

Lafleur, M., B. Fine, E. Sternin, P. R. Cullis, and M. Bloom. 1989. Smoothed orientational order profile of lipid bilayers by ^{2}H-nuclear magnetic resonance. *Biophys. J.* 56:1037–1041.

Macura, S., and R. R. Ernst. 1980. Elucidation of cross relaxation in liquids by two-dimensional N.M.R. spectroscopy. *Mol. Phys.* 41:95–117.

Mayer, L. D., M. J. Hope, P. R. Cullis, and A. S. Janoff. 1985. Solute distributions and trapping efficiencies observed in freeze-thawed multilamellar vesicles. *Biochim. Biophys. Acta.* 817:193–196.

Mazeres, S., V. Schram, J. F. Tocanne, and A. Lopez. 1996. 7-Nitrobenz-2-oxa-1,3-diazole-4-yl-labeled phospholipids in lipid membranes: differences in fluorescence behavior. *Biophys. J.* 71:327–335.

McCabe, M. A., and S. R. Wassall. 1995. Fast-Fourier-transform dePaking. *J. Magn. Reson. B.* 106:80–82.

McIntyre, J. C., and R. G. Sleight. 1991. Fluorescence assay for phospholipid membrane asymmetry. *Biochemistry.* 30:11819–11827.

Nagle, J. F. 1993. Area/lipid of bilayers from NMR. *Biophys. J.* 64: 1476–1481.

Nezil, F. A., and M. Bloom. 1992. Combined influence of cholesterol and synthetic amphiphilic peptides upon bilayer thickness in model membranes. *Biophys. J.* 61:1176–1183.

Pabst, G., M. Rappolt, H. Amenitzsch, and P. Laggner. 2000. Structural information from multilamellar liposomes at full hydration: full *q*-range fitting with high quality x-ray data. *Phys. Rev. E.* 62:4000–4009.

Pastor, R. W., and S. E. Feller. 1996. Time scales of lipid dynamics and molecular dynamics. *In* Biological Membanes. A Molecular Perspective from Computation and Experiment. K. M. Merz and B. Roux, editors. Birkhäuser, Boston. 3–30.

Persson, S., J. A. Killian, and G. Lindblom. 1998. Molecular ordering of interfacially localized tryptophan analogs in ester- and ether-lipid bilayers studied by ^{2}H-NMR. *Biophys. J.* 75:1365–1371.

Petrache, H. I., N. Gouliaev, S. Tristram-Nagle, R. Zhang, R. M. Suter, and J. F. Nagle. 1998. Interbilayer interactions from high resolution x-ray scattering. *Phys. Rev. E.* 57:7014–7024.

Pomorski, T., A. Herrmann, P. Müller, G. van Meer, and K. Burger. 1999. Protein-mediated inward translocation of phospholipids occurs in both the apical and basolateral plasma membrane domains of epithelial cells. *Biochemistry.* 38:142–150.

Pomorski, T., A. Herrmann, A. Zachowski, P. F. Devaux, and P. Müller. 1994. Rapid determination of the transbilayer distribution of NBD-phospholipids in erythrocyte membranes with dithionite. *Mol. Membr. Biol.* 11:39–44.

Pomorski, T., A. Herrmann, B. Zimmermann, A. Zachowski, and P. Müller. 1995. An improved assay for measuring the transverse redistribution of fluorescent phospholipids in plasma membranes. *Chem. Phys. Lipids.* 77:139–146.

Pomorski, T., P. Müller, B. Zimmermann, K. Burger, P. F. Devaux, and A. Herrmann. 1996. Transbilayer movement of fluorescent and spin-labeled phospholipids in the plasma membrane of human fibroblasts: a quantitative approach. *J. Cell Sci.* 109:687–698.

Rance, M., O. W. Sorensen, G. Bodenhausen, G. Wagner, R. R. Ernst, and K. Wuthrich. 1983. Improved spectral resolution in COSY ^{1}H NMR spectra of proteins via double quantum filtering. *Biochem. Biophys. Res. Commun.* 117:479–485.

Seelig, A., and J. Seelig. 1974. The dynamic structure of fatty acyl chains in a phospholipid bilayer measured by deuterium magnetic resonance. *Biochemistry.* 13:4839–4845.

Smeets, E. F., P. Comfurius, E. M. Bevers, and R. F. Zwaal. 1994. Calcium-induced transbilayer scrambling of fluorescent phospholipid analogs in platelets and erythrocytes. *Biochim. Biophys. Acta.* 1195: 281–286.

Sternin, E., M. Bloom, and L. MacKay. 1983. De-Pake-ing of NMR spectra. *J. Magn. Reson.* 55:274–282.

Tang, X. J., M. S. Halleck, R. A. Schlegel, and P. Williamson. 1996. A subfamily of P-type ATPases with aminophospholipid transporting activity. *Science.* 272:1495–1497.

Volke, F., and A. Pampel. 1995. Membrane hydration and structure on a subnanometer scale as seen by high resolution solid state nuclear magnetic resonance: POPC and POPC/$C_{12}EO_4$ model membranes. *Biophys. J.* 68:1960–1965.

Wagner, G., and K. Wüthrich. 1982. Sequential resonance assignments in protein ^{1}H nuclear magnetic resonance spectra. *J. Mol. Biol.* 155: 347–366.

White, S. H., and M. C. Wiener. 1996. The liquid-crystallographic structure of fluid lipid bilayer membranes. *In* Biological Membranes. A Molecular Perspective from Computation and Experiment. K. M. Merz and B. Roux, editors. Birkhäuser, Boston. 127–144.

White, S. H., and W. C. Wimley. 1999. Membrane protein folding and stability: physical principles. *Annu. Rev. Biophys. Biomol. Struct.* 28: 319–365.

Wiener, M. C., and S. H. White. 1992. Structure of a fluid dioleoylphosphatidylcholine bilayer determined by joint refinement of x-ray and neutron diffraction data III. Complete structure. *Biophys. J.* 61: 434–447.

Wimley, W. C., and S. H. White. 1993. Membrane partitioning: distinguishing bilayer effects from the hydrophobic effect. *Biochemistry.* 32:6307–6312.

Yau, W. M., and K. Gawrisch. 2000. Lateral lipid diffusion dominates NOESY cross-relaxation in membranes. *J. Am. Chem. Soc.* 122: 3971–3972.

Yau, W. M., W. C. Wimley, K. Gawrisch, and S. H. White. 1998. The preference of tryptophan for membrane interfaces. *Biochemistry.* 37: 14713–14718.